Evaluation of data sets used to force sea ice models in the Arctic Ocean

J. A. Curry, J. L. Schramm, A. Alam, R. Reeder, and T. E. Arbetter

Program in Atmospheric and Oceanic Sciences, Department of Aerospace Engineering Sciences, University of Colorado, Boulder, Colorado, USA

P. Guest

Department of Meteorology, Naval Postgraduate School, Monterey, California, USA

Received 30 May 2000; revised 8 March 2001; accepted 23 July 2001; published 10 August 2002.

[1] Basin-scale sea ice models are often run uncoupled to either an atmosphere or ocean model to evaluate the sea ice model, to compare different models, and to test changes in physical parameterizations. Such simulations require that the boundary forcing be specified. The specification of atmospheric forcing associated with the surface heat and freshwater fluxes has been done in various sea ice simulations using climatology, numerical weather prediction analyses, or and satellite data. However, the errors in the boundary forcing may be so large that it is difficult to determine whether discrepancies between simulated and observed properties of sea ice should be attributed to deficiencies in the sea ice model or to the boundary forcing. To assess the errors in boundary forcing, we use data from the Surface Heat Budget of the Arctic Ocean (SHEBA) to evaluate various data sets that have been used to provide boundary forcing for sea ice models that are associated with the surface heat and freshwater fluxes. The impact of errors in these data sets on a sea ice model is assessed by using a single-column ice thickness distribution model, which is alternately forced with in situ measurements from SHEBA and output from large-scale analyses. Substantial discrepancies are found among the data sets. The response of the sea ice model to the different forcing data sets was considerable. *INDEX TERMS:* 4504 Oceanography: Physical: Air/sea interactions (0312); 4540 Oceanography: Physical: Ice mechanics and air/sea/ice exchange processes; 3307 Meteorology and Atmospheric Dynamics: Boundary layer processes; *KEYWORDS:* sea ice, arctic ocean, air/ice interactions, SHEBA

1. Introduction

[2] Large-scale sea ice models are used for operational forecasting of sea ice characteristics, for understanding physical processes, and in studying climate variability. For these applications, large-scale sea ice models may be run in stand-alone mode, coupled to a large-scale ocean model, or included in a coupled climate model. Basin-scale sea ice models are often run in stand-alone mode to evaluate the sea ice model, compare different models, and evaluate changes in physical parameterizations. Such simulations require that the boundary forcing be specified. One of the great difficulties in development and evaluation of large-scale sea ice models has been the absence of suitable data for forcing and evaluation of the model. When discrepancies in the simulated sea ice are found, it is unclear whether the discrepancies arise from model deficiencies or from deficiencies in the forcing data set.

[3] Atmospheric boundary forcing for sea ice models consists of wind stress, freshwater flux, and surface heat fluxes. In the case of surface turbulent fluxes, typically, the atmospheric surface wind, temperature, and humidity are specified, and the fluxes are calculated interactively using the modeled surface temperature. Earlier simulations used monthly averaged atmospheric forcing derived from climatologies [e.g., *Hibler*, 1979; *Holland et al.*, 1993]. In the Arctic Ocean, fairly accurate large-scale wind fields are produced by numerical weather prediction analyses owing to the assimilation of surface pressure buoy data. The specification of daily varying atmospheric forcing associated with the surface heat and freshwater fluxes has been done in various simulations using numerical weather prediction analyses [e.g., *Chapman et al.*, 1994; *Arbetter et al.*, 1999; *Hilmer et al.*, 1998] or from analyses of conventional data [*Zhang et al.*, 1998]. However, the surface heat and freshwater fluxes determined from these sources show substantial discrepancies and are overall less reliable than the surface momentum fluxes (which are fairly accurate owing to the assimilation of surface pressure buoy data). This has caused numerous sea ice modelers to use numerical weather prediction (NWP) winds and surface air temperature but climatological values for surface radiation fluxes, surface air humidity, and precipitation [e.g., *Harder et al.*, 1998; *Kreyscher et al.*, 2000]. *Arbetter et al.* [1999] used National Centers for Environmental Prediction (NCEP)

0148-0227/02/2000JC000466$09.00

reanalyses [*Kalnay et al.*, 1996] as forcing data, but the surface radiation fluxes were multiplied by a factor to bring them closer to climatological values.

[4] Several comparisons of numerical weather prediction analyses and satellite products with climatology or limited in situ observations have been conducted that are relevant to assessing the suitability of these data sets for forcing sea ice models. While there have been several comparisons of individual flux components determined by numerical weather prediction models with observations, there has not been a systematic evaluation of the utility of numerical weather prediction analyses for forcing sea ice models.

[5] A number of studies have addressed the precipitation P and surface evaporation E over the Arctic Ocean from numerical weather prediction analyses (note that no attempt has been made to determine either of these quantities from satellite). *Serreze and Hurst* [2000] found that both the NCEP and European reanalysis (ERA) capture the major spatial features of annual mean precipitation and general aspects of the seasonal cycle but with some notable errors. Both underestimate precipitation over the Atlantic side of the Arctic. NCEP overestimates annual totals over the central Arctic Ocean. Overall, the ERA predictions are better. Both models perform best during winter and worst during summer. *Cullather et al.* [2000] found that forecast $P - E$ for 70°–90°N is very small compared to climatology ($\sim$11–13 cm yr^{-1} versus $\sim$19 from climatology). In particular, the NCEP forecast of E is about twice as large as that computed from Soviet surface latent heat flux climatologies.

[6] Several studies have compared surface radiation data sets derived from numerical weather prediction analyses and satellites with Russian ice island data. *Zhang and Rothrock* [1996] compared surface radiation fluxes over the Arctic Ocean from the European Centre for Medium-Range Weather Forecasts (ECMWF), Reading, England and NCEP analyses, satellite analyses from *Schweiger and Key* [1994] and *Pinker et al.* [1995], empirical parameterizations using cloud and surface air temperature climatologies [*Zillman*, 1972; *Idso and Jackson*, 1969], and Russian ice island observations [*Marshunova*, 1961]. The range of monthly average fluxes among the different data sets was 40 W m^{-2} for downwelling longwave fluxes and $\sim$100 W m^{-2} during mid-June for downwelling shortwave fluxes. A large portion of this variation was associated with different estimates of cloud properties. *Serreze et al.* [1998] found that NCEP shortwave fluxes were consistently too high and longwave fluxes were consistently too low (indicative of too little cloud); International Satellite Cloud Climatology Project (ISCCP)-derived fluxes were closer in magnitude to the ice island observations. NCEP and ISCCP products captured 50–60% of the observed spatial variance in global radiation during most months. *Serreze and Hurst* [2000] found that the ERA values of surface radiation fluxes were much closer to climatological values than were the NCEP values.

[7] The Surface Heat Budget of the Arctic Ocean (SHEBA) experiment [*Perovich et al.*, 1999] has provided arguably the highest-quality and most comprehensive suite of surface flux measurements ever made in the Arctic Ocean. This data set has already been used to evaluate several aspects of the ECMWF analysis products. Of direct relevance to forcing sea ice models, C. Bretherton et al. (unpublished manuscript, 2000) compared the surface downwelling longwave flux and precipitation, which is of direct relevance to forcing sea ice models. It was found that the monthly averaged precipitation values compared well, although specific events were not accurately determined by ECMWF and there were several events that were anomalously high. ECMWF surface air temperature is significantly too warm, especially during winter. ECMWF downwelling longwave radiation fluxes were accurately modeled during clear periods and during summer. During some cloud winter and spring periods the daily average modeled longwave radiation is up to 50 W m^{-2} lower than observed. *Beesley et al.* [2000] found that during November the ECMWF surface air temperature fluctuations were dramatically damped relative to the SHEBA observations, creating 10–15 K errors in surface air temperature, particularly under clear, calm conditions.

[8] A critical issue in assessing the atmospheric data for forcing sea ice models is the sensitivity of these sea ice models to errors in the various forcing parameters. Several studies have addressed the impact of errors in atmospheric forcing on sea ice simulations. *Arbetter et al.* [1997] compared the sensitivity to surface heat flux perturbations of one-dimensional (1-D) slab thermodynamic models, single-column ice thickness distribution models, and 2-D dynamic/thermodynamic sea ice models. It was found that the dynamic/thermodynamic sea ice models and ice thickness distribution models are substantially less sensitive to surface heat flux perturbations than are the 1-D slab thermodynamic models. The sensitivity of the single-column ice thickness distribution models is within the range of the 2-D dynamic/thermodynamic models that use different rheologies. *Flato* [1996] found that a 2-D ice thickness distribution model was more sensitive to heat flux perturbations than was a 2-D model with slab thermodynamics, approaching the sensitivity of some of the 1-D models. *Flato and Hibler* [1995] and *Schramm et al.* [1997b] showed that inclusion of an ice thickness distribution results in increased sensitivity to variations in snowfall relative to the simple 1-D slab thermodynamic models [e.g., *Maykut and Untersteiner*, 1971].

[9] Another critical issue in the forcing of sea ice models is the time resolution of the forcing (monthly versus daily versus resolving the diurnal cycle). An additional issue that needs to be considered is the importance of timing in key meteorological events at times when the sea ice is especially vulnerable to atmospheric forcing. Examples of such events noted at SHEBA included (1) the May 29 rainfall event (relatively early in the season) that initiated melt metamorphism of the snowpack and heralded the onset of the melt seasonand (2) the storm at the end of July/beginning of August that dramatically increased the open water fraction when the sea ice was most vulnerable to divergence. Such events have irreversible effects on the sea ice; averaging or mistiming of these events may have a substantial impact on its seasonal evolution.

[10] This paper presents an evaluation of several different atmospheric forcing data sets that are being used as boundary forcing for sea ice models, including numerical weather prediction analyses. Observations from the SHEBA field experiment are used as ''truth'' in the evaluation. We focus here specifically on the forcing associated with the heat and freshwater fluxes owing to the large discrepancies

Table 1. Monthly Averages of Surface Atmospheric Variables for SHEBA, October 1997 through September 1998

Month	Wind Speed, m s^{-1}	Temperature, K	Humidity, g kg^{-1}	Shortwave Flux, W m^{-2}	Longwave Flux, W m^{-2}	Precipitation, mm d^{-1}
Oct.	3.7	255.5	0.78	6.6	227.9	0.17
Nov.	5.2	251.9	0.67	1.6	207.5	0.31
Dec.	4.8	240.4	0.20	0.0	149.1	0.11
Jan.	5.2	242.4	0.27	0.0	169.3	0.65
Feb.	4.6	241.	0.23	17.0	153.0	0.19
March	4.9	250.5	0.57	58.0	205.2	0.43
April	5.1	255.0	0.79	147.2	218.3	0.48
May	4.9	261.7	1.46	248.9	244.7	0.31
June	4.9	272.4	3.41	281.9	278.7	0.44
July	4.4	273.2	3.74	207.3	299.2	1.11
Aug.	5.1	272.3	3.54	113.2	299.1	0.89
Sept.	4.5	268.8	2.59	37.6	280.1	0.67

in the available data sets and the suitability of the SHEBA data set for evaluation of these fluxes. The impact of errors in these data sets on a sea ice model is assessed by using a single-column ice thickness distribution model, which is alternately forced with in situ measurements from SHEBA, numerical weather prediction analyses, and the Polar Exchange at the Sea Surface (POLES) analyses.

2. Description and Evaluation of Data Sets

[11] To specify the atmospheric forcing for a sea ice model, the following parameters are required: (1) surface downwelling longwave and shortwave radiation fluxes, (2) surface air temperature and humidity, (3) surface wind speed and direction, and (4) precipitation. Note that the surface turbulent fluxes are not specified; typically, in sea ice models these are calculated using the simulated surface temperature and surface roughness. Also, the net radiative flux is determined using the simulated surface temperature and albedo.

[12] There are three general options for forcing a sea ice model with atmospheric data: (1) numerical weather prediction analyses (e.g., ECMWF and NCEP), (2) satellite-derived fluxes or flux input variables, and (3) other analyses that are based primarily on conventional observations (e.g., surface buoys) or climatological data sets. This study focuses on data sets with high resolution (at least daily) and considers specifically the NCEP and ERA reanalysis products and also a hybrid data set, the POLES sea ice model forcing data set. These data are evaluated using in situ observations obtained during SHEBA.

2.1. Data Set Descriptions

[13] The data used to evaluate the atmospheric parameters required to force a sea ice model are obtained from the SHEBA project [*Perovich et al.*, 1999]. The SHEBA observations were made during the period October 2, 1997 to October 10, 1998. The Canadian coastguard ice breaker *Des Groseilliers* was deployed in a multiyear ice floe at 75°16.3′N, 142°41.2′W. Over the course of the field study the SHEBA ice camp drifted considerably northwestward, reaching 80°N, 162°W by the end of the experiment.

[14] Measurements of surface radiation fluxes and surface air temperature, humidity, and winds were obtained at multiple levels from the a 20-m flux tower operated by the SHEBA surface flux group [*Andreas et al.*, 1999] and from instruments on two 10-m meteorological towers operated by the SHEBA project office (R. Moritz, personal communication, 1998). Radiation fluxes were measured using Eppley pyranometers and pyrgeometers near the surface. Daily precipitation accumulation was measured using a Nipher shielded snow gauge system, which has been corrected for blowing snow (R. Moritz, personal communication, 1999). Measurement errors were minimized by comparing measurements at different levels on the flux tower. Errors in the SHEBA data set (expressed as 95% confidence interval) are estimated to be 0.1°C for air temperature, 4% for relative humidity, and 6% + 0.5 m s^{-1} for the wind vector. When the air temperature was below −20°C, the uncertainty of the relative humidity increased to ∼10%. An intercomparison of different Eppley radiometers plus preexperiment and post-experiment calibration indicates errors of 5 W m^{-2} for both longwave and shortwave radiation, although this error may be larger if compared to an absolute standard.

[15] Reanalysis products are not yet available for the SHEBA year from ECMWF, although a second reanalysis is being conducted by ECMWF during summer 2000 which will include the SHEBA period. Hence the operational forecasts and analyses from NCEP and ECMWF are used here. Specifically, we use the surface data from the NCEP/National Center for Atmospheric Research (NCAR) reanalysis product, which has a spatial resolution of 2.5° latitude and longitude and 6 hours. The ECMWF cooperated closely with SHEBA to provide a special analysis data set with hourly resolution (Bretherton et al., unpublished manuscript, 2000).

[16] The POLES sea ice model forcing data set [*Zhang et al.*, 1998] is available daily at a spatial resolution of 160 km over the Arctic Ocean from 1979 to 1998 (see also http://iabp.apl.washington.edu). This data set uses observations from the International Arctic Buoy Programme (IABP) to estimate daily values of u and v components of geostrophic wind. The surface air temperature data set [*Rigor et al.*, 2000] uses a sophisticated optimum interpolation technique to derive twice daily values from buoys, manned drifting stations, and meteorological land stations. Surface radiation fluxes are determined following *Zhang and Rothrock* [1996], who use the empirical parameterizations of *Zillman* [1972] and *Idso and Jackson* [1969] with inputs from cloud climatology and the surface air temperature data set. This data set has been used in our

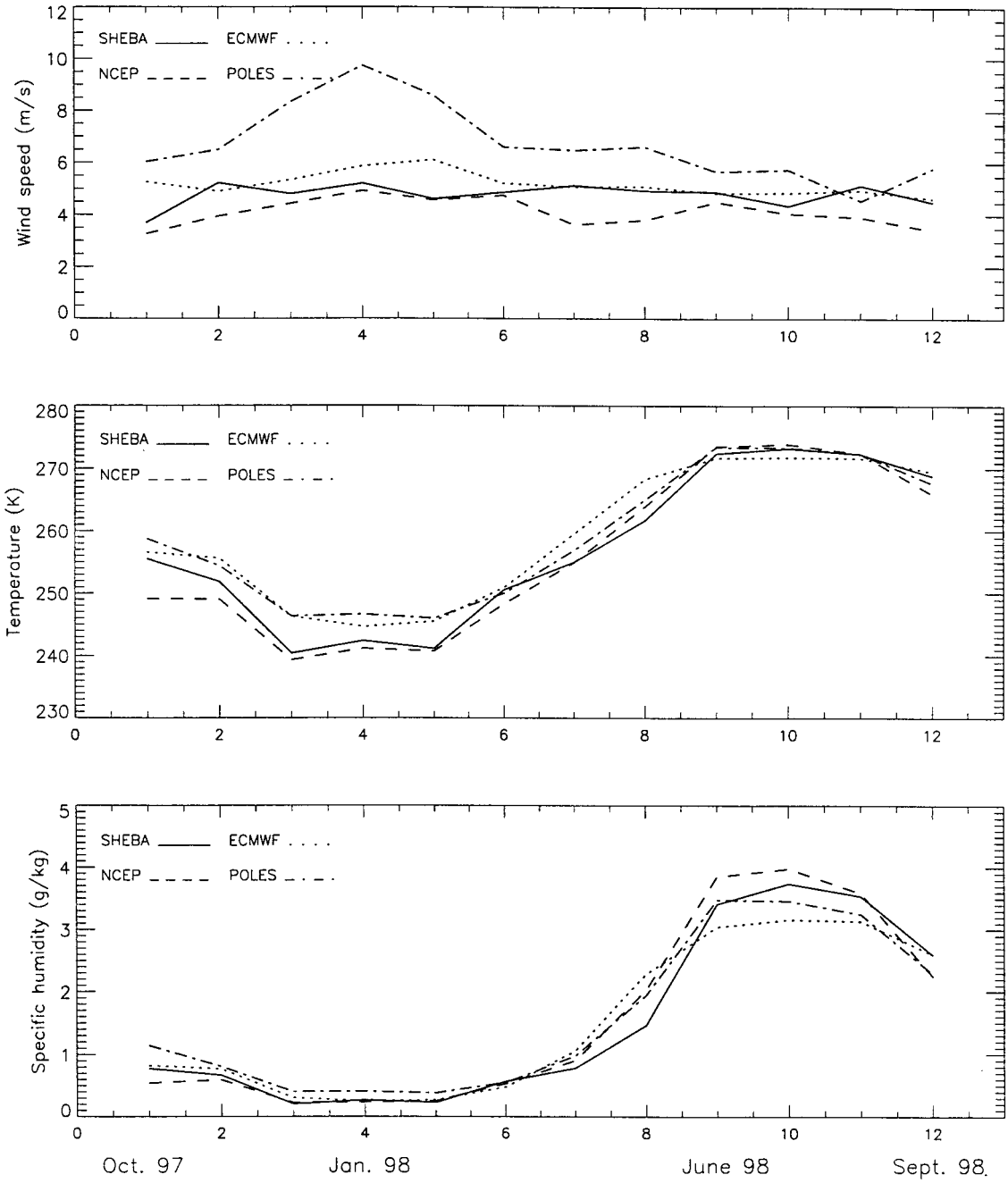

Figure 1. Comparison of monthly averaged values using the SHEBA field observations, ECMWF analyses, NCEP analyses, and POLES data for surface wind speed, surface air temperature, surface air humidity, surface downwelling shortwave radiation flux, surface downwelling longwave radiation flux, and precipitation.

research by *Arbetter* [1999] by supplementing the data set with the precipitation climatology of *Serreze and Hurst* [2000], based upon a gridded product with measurements from Russian drifting stations and gauge corrected station data for Eurasia and Canada.

2.2. Comparison With SHEBA Data

[17] The monthly averaged values of surface wind speed, air temperature and humidity, downwelling shortwave and longwave fluxes, and precipitation observed at SHEBA are given in Table 1. When these values are compared with climatological values of observations for the Arctic Ocean previously used to force thermodynamics (such as compiled by *Ebert and Curry* [1993] for 80°N), the following significant differences are found. The shortwave fluxes at SHEBA are somewhat lower than the climatological values (the SHEBA values correspond to latitudes between 75° and 80°N). Surface air temperatures during SHEBA were somewhat colder than climatology during winter but slightly warmer during March and April.

[18] A comparison of the NCEP, ECMWF, and POLES analyses with SHEBA data is shown in Figure 1 and Table 2.

Table 2. Comparison of ECMWF, NCEP, and POLES Analyses With SHEBA Observations for Each of the Four Seasons

		10-m Wind Speed, m s^{-1}			2-m Air Temp, K			2-m Specified Humidity, g kg^{-1}			Shortwave Radiation, W m^{-2}			Longwave Radiation, W m^{-2}			Precipitation, mm d^{-1}		
		ECMWF	NCEP	POLES	ECMWF	NCEP	POLES	ECMWF	NCEP	POLES	ECMWF	NCEP	POLES	ECMWF	NCEP	POLES	ECMWF	NCEP	POLES
OND	bias	0.31	−0.76	2.43	5.21	−1.67	4.8	0.14	0	0.23	3.76	3.99	−2.14	−14.43	−14.32	32.4	0.24	0.45	0.18
	rmse	1.45	1.76	3.59	6.75	3.62	6.49	0.26	0.14	0.32	4.43	4.2	1.72	22.38	22.92	45.37	0.87	0.99	0.4
	corr	0.86	0.81	0.74	0.81	0.92	0.81	0.75	0.9	0.7	0.26	0.73	0.62	0.93	0.91	0.77	0.41	0.43	0.05
JFM	bias	0.79	−0.17	3.37	2.04	−1.53	2.57	−0.03	−0.02	0.08	16.23	20.62	−21.69	−18.09	−18.06	27.34	−0.13	0.05	−0.1
	rmse	1.73	1.41	4.52	5.56	3.08	5.52	0.21	0.1	0.22	26.79	31.04	23.15	29.13	27.01	46.56	1.94	2.02	1.37
	corr	0.76	0.84	0.42	0.74	0.94	0.78	0.72	0.94	0.68	0.75	0.79	0.74	0.88	0.91	0.69	0.56	0.25	0.04
AMJ	bias	0.03	−1.01	1.27	3.09	0.69	1.66	0.17	0.3	0.17	23.92	63.22	−9.51	−8.51	−31.09	6.95	0.09	0.09	−0.02
	rmse	0.96	1.52	3.49	5.01	1.95	3.28	0.51	0.33	0.37	45.55	76.47	43.34	32.75	38.24	30.34	1.11	0.92	0.78
	corr	0.88	0.79	0.46	0.86	0.98	0.93	0.92	0.99	0.96	0.86	0.87	0.84	0.73	0.88	0.65	0.21	0.26	−0.01
JAS	bias	0.14	−0.86	0.71	−0.19	−0.38	0.01	−0.25	0.08	−0.2	19.56	78.64	26.56	−2.88	−37.16	−16.67	0.23	−0.04	−0.03
	rmse	1.19	1.61	2.4	1.54	2.74	1.51	0.47	0.4	0.4	42.85	91.64	26.56	15.94	41.05	21.52	2.98	3.21	2.93
	corr	0.87	0.81	0.6	0.85	0.9	0.87	0.87	0.94	0.89	0.89	0.91	0.9	0.63	0.58	0.61	0.24	0.04	−0.06

In Figure 1, monthly averaged values of surface wind speed, air temperature and humidity, downwelling shortwave and longwave fluxes, and precipitation are given to illustrate the annual cycle of the biases. In Table 2, seasonal statistics (bias, RMS error, and correlation) are given for daily averaged values.

[19] The wind speed comparisons shows that during winter the POLES values are substantially larger than the observations. The POLES values correspond to geostrophic winds associated with the surface pressure field. The NCEP and ECMWF winds show seasonal biases that are <1 m s^{-1} and correlations that are $\sim$0.8. Overall, the statistics for the ECMWF winds are slightly better than for the NCEP winds.

[20] The surface air temperature comparisons show that both ECMWF and POLES are substantially warmer than observed values during autumn and winter. NCEP values are much closer to observations but biased slightly cooler. Overall, the NCEP surface air temperatures are more accurate.

[21] When interpreting the biases in surface air humidity, it should be noted that wintertime specific humidity values are smaller than summertime values by an order of magnitude. Except for the spring season, the NCEP values are quite close to the observations, as indicated by low biases, RMS error, and high correlations.

[22] Comparison of the shortwave radiation fluxes shows that NCEP values are systematically too large; the bias is as high as 78 W m^{-2} during the summer months. The POLES and ECMWF values have smaller bias errors than NCEP. The POLES and NCEP biases are similar in magnitude but opposite in sign except for the summer season (when both are biased high). Comparisons of the longwave radiation fluxes show that POLES values are biased significantly high during autumn and winter, while NCEP is biased significantly low during spring and summer. Overall, the ECMWF longwave radiation fluxes have the best statistics. In terms of net downwelling radiation fluxes, both the ECMWF and POLES have similar biases in annually averaged net downwelling radiation fluxes, with the NCEP bias significantly higher.

[23] Comparisons of the precipitation values with SHEBA observations show little bias for each of NCEP, ECMWF, and POLES analyses. However, the correlations are quite low, indicating that these analyses are not able to capture the daily variations in precipitation.

[24] These comparisons suggest the following about the NCEP, ECMWF, and POLES analyses. The POLES data compared well with observations except for the surface wind speeds. The good comparison of the *Serreze and Hurst* [2000] precipitation climatology with SHEBA observations indicates that the SHEBA year was typical in terms of precipitation. The variables from NCEP analyses showed reasonable agreement with SHEBA data for all data parameters except for the radiation fluxes. The biases in the NCEP radiation fluxes are consistent with insufficient clouds predicted by the model. The ECMWF values compare quite well with the SHEBA observations except for a high bias in surface air temperature.

3. Impact of Forcing Data Sets on Sea Ice Simulations

[25] To examine the extent to which errors in the surface fluxes result in variations in the simulated sea ice properties, we use a single-cell ice thickness distribution model [*Schramm et al.*, 1997a; *Holland and Curry*, 1999; *Curry et al.*, 2001] that is alternately forced with in situ measurements from SHEBA and corresponding analyses from NCEP, ECMWF, and POLES. The sea ice model used in this study is a Lagrangian single-cell ice thickness distribution model that responds to both thermodynamical and dynamical forcing [*Schramm et al.*, 1997a; *Holland and Curry*, 1999]. The model allows for a specified number of level and ridged ice categories within the model domain. Divergent sea ice motion causes sea ice to be exported from the model domain, whereas convergent motion causes ice ridging to occur. Shearing of the ice pack causes both open water and pressure ridges to form. Parameterization of these processes is done using a redistributor function that reorganizes the ice in the model domain based on the kinematic forcing. The different ice thickness categories are described by a variety of properties including age, salinity, snow cover, and melt pond cover. Each ice thickness category is thermodynamically independent from one another with different interfacial heat fluxes being computed for each ice category. Spectral radiative transfer through the ice and open water is included. An explicit melt pond parameterization is included in the model, whereby a specified fraction of meltwater is allowed to run off or drain into the ocean, and the remainder of the water pools into melt ponds. The sea ice model is coupled to an ocean mixed layer model.

[26] The model has been updated from the *Curry et al.* [2001] SHEBA simulations to include a new melt pond parameterization, which was motivated by the complexity of the original *Ebert and Curry* [1993] pond parameterization and its poor performance against the SHEBA data. The new melt pond parameterization is described as follows. Initially, ponds arise from the snowmelt water reservoir that is converted into melt pond volume when snow disappears from an ice thickness category. The pond water is partitioned into depth and areal fractions using a diagnostic aspect ratio derived from SHEBA data [*Perovich et al.*, 2002], $h_p = 0.8\ P$ for multiyear ice and $h_p = 0.2\ P$ for first-year ice, where P is pond areal fraction, h_p is pond depth (in meters), and V_p is a fractional pond volume, (in meters), defined by $V_p = h_p p$. Hence the determination of pond volume along with the specified aspect ratio between pond volume and depth is sufficient to determine the pond volume and depth. A runoff fraction of 0.85 is specified. Pond volume for each ice thickness category changes owing to any melt occurring over the nonponded ice or any melting or freezing of the ponded ice as a result of the net energy balance over ponds and any precipitation over the ponded area (see *Ebert and Curry* [1995] and *Schramm et al.* [1997a] for details of the sea ice and melt pond optics). If pond depth is greater than the ice thickness of that category, the pond is converted to lead, and the pond fraction is added to the lead fraction. The single-column ice model is initialized using the ice thickness distribution determined from submarine sonar (Scientific ice expedition, D. Rothrock, personal communication, 2000), which determined the average ice thickness of the SHEBA floe to be 1.5 m in September 1997. Daily ice deformation (used to force the dynamics of the model) is determined from the analysis of *Lindsay* [2002]. Thermal forcing is alternately specified

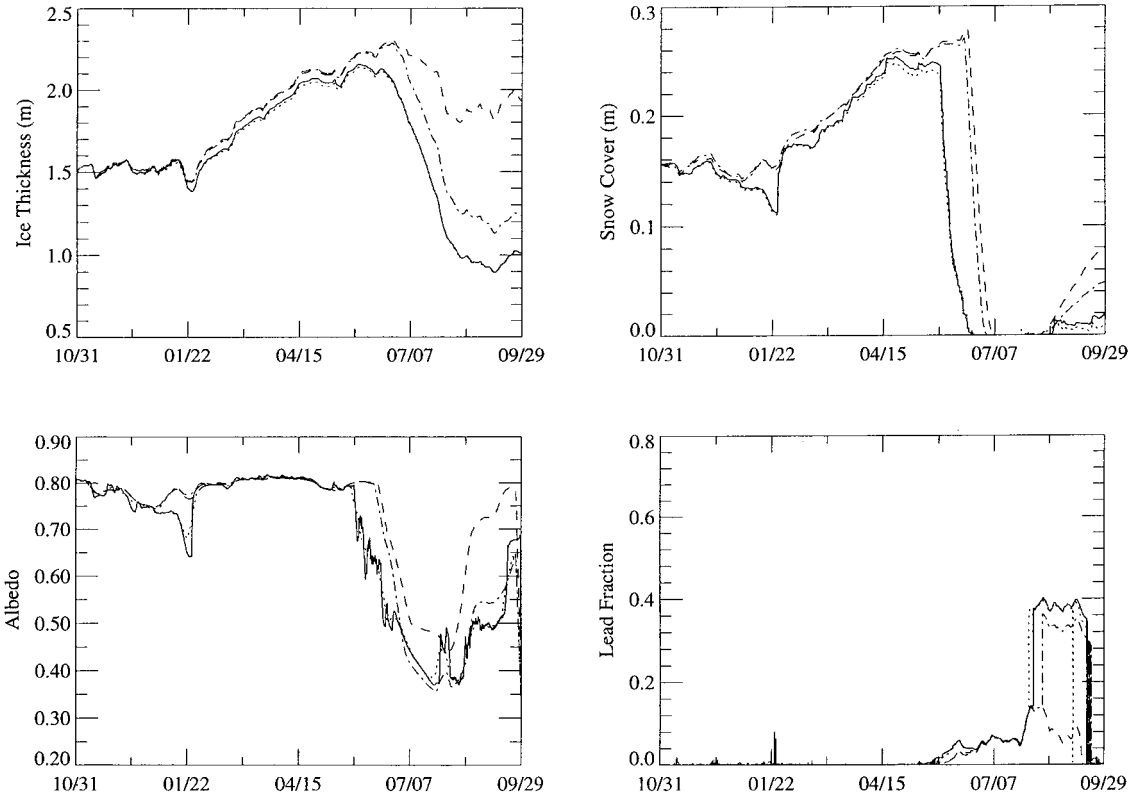

Figure 2. Comparison of simulated values over the SHEBA annual cycle of average ice thickness, snow depth, surface albedo, and lead fraction for different resolutions of the forcing data using the SHEBA field observations. Hourly forcing and time step, solid curves; 6-hour instantaneous forcing and time step, dotted curves; daily averaged forcing with 6-hour time steps, dashed curves; and monthly averaged forcing splined to 6-hour resolution with 6-hour time steps, dash-dotted curves.

using the SHEBA in situ measurements and the corresponding NCEP, ECMWF, and POLES analyses.

[27] In evaluating the impact of errors in the atmospheric forcing data on a sea ice model, it is important to consider the varying sensitivities of different sea ice models to perturbations in atmospheric forcing. On the basis of the model comparisons conducted by *Arbetter et al.* [1997] we judge that the single-column ice thickness distribution is fairly representative of sea ice models presently used for climate applications in its overall sensitivity to surface flux perturbations.

3.1. Temporal Resolution of Atmospheric Forcing Data

[28] The different atmospheric forcing data sets have different temporal resolutions. The ECMWF analyses have hourly resolution (note this is a special data set for SHEBA; ECMWF analyses typically have 6-hour resolution); the NCEP analyses have 6-hour resolution, and the POLES data set has daily resolution. Different sea ice simulations have used different time steps and different resolutions of the forcing data. This range is illustrated by *Schramm et al.* [1997a], who used 8-hour time steps and forcing data that were splined from monthly averaged values, *Arbetter et al.* [1999], who used daily averaged forcing and 6-hour time steps, *Arbetter* [1999], who used 6-hour time step and forcing data, and *Curry et al.* [2001], who used hourly time steps and forcing data.

[29] These different time steps and temporal resolutions for atmospheric forcing may influence the simulation results. To examine this influence, we use the observed SHEBA data to force the sea ice model in four different ways: (1) 1-hour forcing and time step, (2) 6-hour instantaneous forcing and time step, (3) daily averaged forcing with 6-hour time step, and (4) monthly averaged data splined to 6-hour resolution and 6-hour time step.

[30] Simulations of the SHEBA annual cycle using these different time steps and temporal resolution are shown in Figure 2. *Curry et al.* [2001] compare the simulation with hourly forcing and time step with observations obtained during SHEBA. The simulations compared reasonably well with observations, with the following noted deficiencies. When compared with observations, the modeled ice thickness decreases over the annual cycle by 60 cm, while the observations show a decrease of 45 cm. The modeled snow melts too rapidly during spring. The model produces a minimum summer melt albedo of 52%, compared with an observed minimum value of 39%. This arises because the simulated melt pond fraction is too small and the pond depth is too shallow. The new melt pond parameterization results shows excellent comparison with SHEBA observations and produces a minimum albedo of 39% [see *Arbetter*, 1999].

[31] Figure 2 shows significant differences among the different simulations, particularly for the monthly averaged

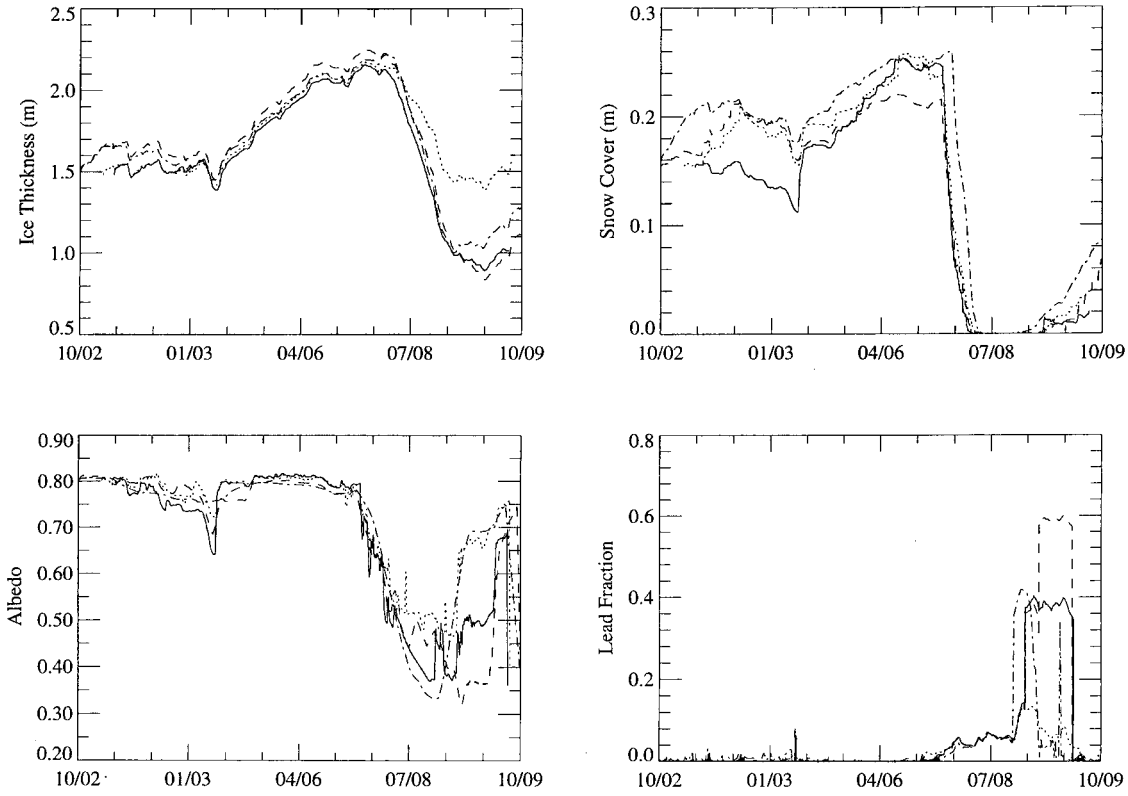

Figure 3. Comparison of simulated values over the SHEBA annual cycle of average ice thickness, snow depth, surface albedo, and lead fraction for different atmospheric forcing data sets. SHEBA field observations, solid curves; ECMWF analyses, dotted curves; NCEP analyses, dashed curves; and POLES data, dash-dotted curves.

forcing that is splined to 6-hour resolution. At the end of the SHEBA year the average ice thickness was 1.5 m for the 1-hour forcing, with the 6-hour instantaneous and daily averaged forcing within 10 cm of this value. However, the simulation with monthly averaged forcing produces 1.9 m of ice at the end of the year. The monthly averaged forcing shows substantially more snow cover in June than do the other simulations, and the snow accumulates much more rapidly during September. During the transition seasons, detailed timing of the snow accumulation is important because of its impact on the surface energy exchange during these transitional periods with rapid changes. The smaller melt season in the simulation with monthly averaged forcing results in significantly higher summertime surface albedos, which causes the thicker ice. The thicker ice and lower surface albedo are also reflected in the relatively low lead fraction during August.

[32] Although the 1-hour and 6-hour instantaneous and daily averaged forcing with 6-hour time step show little difference in ice thickness and snow depth, some interesting differences are noted in surface albedo and lead fraction for the daily averaged forcing. These differences are most apparent after mid-July, when the average ice thickness has diminished to $\sim$1 m and the lead fraction is rapidly increasing in response to a storm. The daily averaged forcing results in a significantly lower surface albedo during summer. The lower albedo values in late June through mid-July arise from more meltwater forming because of the absence of a diurnal cycle in solar radiation. The lower albedo then results in more ice melting and a larger lead fraction in August.

3.2. Comparison of Different Surface Forcing Data Sets

[33] Figure 3 compares the simulated annual cycles using SHEBA observations (1-hour resolution and time step), ECMWF (1-hour resolution and time step), NCEP (6-hour resolution and time step), and POLES (1-day resolution and time step). There are several notable differences among the simulations. ECMWF shows a relatively high summertime surface albedo, low lead fraction during August, and relatively thick ice at the end of the annual cycle. NCEP shows high lead fraction and low surface albedo during August. POLES shows relatively low surface albedo during July but diminished lead fraction and enhanced snow accumulation in August and September. These differences can be related to differences in surface forcing (as well as time step) as follows.

[34] NCEP lead fraction during August and September is high (and the surface albedo is low) owing to the high bias in NCEP net surface downwelling radiation flux during this period. In spite of the NCEP high bias during July as well the NCEP surface albedo shows fairly good agreement with the baseline SHEBA simulation and, if anything, is slightly higher than the baseline simulation. In late June and early July the relatively large NCEP net downwelling radiation flux is compensated by a relatively low amount of meltwater from snow, producing melt pond fraction and surface albedo that is similar to the SHEBA baseline forcing.

Around July 17, NCEP analyses produce strong cooling (note there was an observed clear event at this time), which resulted in freezing of the ponds and a corresponding increase in surface albedo.

[35] ECMWF shows a relatively high summertime surface albedo, which is related directly to relatively small amount of melt ponds that form. The ECMWF snow depth at the end of May is very close to the baseline SHEBA simulations, and the ECMWF net downwelling surface radiation flux in July is slightly high relative to the observed SHEBA values (Figure 1). The reason that ECMWF melt ponds show little development appears to be associated with the relatively low ECMWF summertime values of surface air temperature and humidity, which results in high values of sensible and latent heat fluxes that cool the surface. This surface cooling is sufficient to cause nocturnal freezing of the ponds, diminishing their development. The overall thicker ice and high amount of snowfall in August result in a much smaller lead fraction during August.

[36] The POLES simulation produces slightly lower albedos during late June and July than does the baseline SHEBA simulation. This appears to arise from a combination of enhanced meltwater from the larger snow accumulation, slightly positive net downwelling radiation flux, and the 1-day time step that diminishes the possibility of nocturnal freezing of melt ponds. The greatest difference between the POLES and the baseline SHEBA simulation is the timing of the freeze-up of the leads, which occurs in mid-August for the POLES forcing, owing to a negative bias in net downwelling radiative flux (inferred from Figure 1) and relatively heavy snowfall in August.

4. Summary and Conclusions

[37] This study has evaluated different atmospheric data sets used for forcing sea ice models, focusing on data sets that have at least daily resolution. Specifically, the following data parameters were examined: (1) surface wind speed, (2) surface air temperature, (3) surface air humidity, (4) downwelling longwave radiation flux, (5) downwelling shortwave radiation flux, and (6) precipitation. The data sets that were evaluated were NCEP, ECMWF, and POLES analyses. These data sets were evaluated against the SHEBA data, which were obtained from a drifting ice station during the period October 1997 through October 1998. Comparison of these data sets shows the following. The POLES data compared well with observations except for the surface wind speeds. Recent efforts to convert the POLES geostrophic winds to actual 10-m wind speeds (J. Francis, personal communication, 2000) should improve this. The variables from NCEP analyses showed reasonable agreement with SHEBA data for all data parameters except for the radiation fluxes. The biases in the NCEP radiation fluxes are consistent with insufficient clouds predicted by the model. The ECMWF values compare quite well with the SHEBA observations except for a high bias in surface air temperature and humidity. With a new surface albedo parameterization being incorporated into the ECMWF model, surface temperature predictions are more accurate (M. Miller, personal communication, 1999).

[38] The impact of errors in these data sets on a sea ice model is assessed by using a single-column ice thickness distribution model, which is alternately forced with in situ measurements from SHEBA and the NCEP, ECMWF, and POLES analyses. The simulation using ECMWF forcing shows a relatively high summertime surface albedo, low lead fraction during August, and relatively thick ice at the end of the annual cycle. The simulation using NCEP forcing shows high lead fraction and low surface albedo during August. The simulations using POLES forcing show relatively low surface albedo during July but diminished lead fraction and enhanced snow accumulation in August and September. These differences were related to differences in surface forcing as well as to the temporal resolution of the forcing. The most critical aspects of the surface forcing appear to be the late spring and late summer snowfall (amount and timing), midsummer cooling events (either nocturnal, storms, or clear sky events) that result in the freezing of melt ponds, and bias in summertime net downwelling radiation flux.

[39] It is not entirely clear to what extent the results of this study can be generalized to infer the suitability of the NCEP, ECMWF, and POLES analyses for forcing large-scale sea ice models. In simulation of a single annual cycle, the effects of long-term biases do not have sufficient time to accumulate and the differences in simulations might be much larger if long-term or equilibrium simulations were conducted. On the other hand, the differences between the simulations found here might be larger than for simulations of thicker ice and using a less complicated model. The relatively thin ice at SHEBA (at least 1 m thinner than expected from sea ice thickness climatologies in this region) makes the simulations more sensitive to surface heat flux perturbations or errors. The complex surface albedo parameterization and explicit treatment of melt ponds in the model used here produces a stronger ice-albedo feedback than models with simpler treatments of these processes [e.g., *Curry et al.*, 1995, 2001]. Additional studies testing different forcing data sets (for both the Arctic and Antarctic) for a hierarchy of model types and for longer a simulation period are needed to definitively address this issue. However, observations on this timescale and space scale are presently lacking to evaluate such sea ice model simulations.

[40] **Acknowledgments.** This research was funded by several grants from NSF-OPP and by DOE ARM. We thank our colleagues in the SHEBA Atmospheric Surface Flux Group, E. Andreas, C. Fairall, and O. Persson for help collecting and processing the data. We would like to thank R. Moritz and the SHEBA project office for providing the precipitation data. We would like to thank D. Rothrock for providing the ice thickness distribution data for SHEBA. We would like to thank R. Lindsay for providing the sea ice deformation data. We would like to thank C. Jakob and C. Bretherton for their efforts in assembling the special ECMWF data set for SHEBA. We would like to thank J. Zhang for extending the POLES to include the SHEBA year at our request. The NCEP/NCAR analyses were obtained from the archive at NCAR. We would also like to thank M. Serreze for providing us with the precipitation climatology.

References

Andreas, E. L., C. W. Fairall, P. S. Guest, and P. O. G. Persson, An overview of the SHEBA atmospheric surface flux program, paper presented at 5th Conference on Polar Meteorology and Oceanography, Am. Meteorol. Soc., Dallas, Tex., Jan. 10–15 1999.

Arbetter, T. E., J. A. Curry, M. M. Holland, and J. A. Maslanik, Response of sea ice models to perturbations in surface heat flux, *Ann. Glaciol.*, *25*, 193–197, 1997.

Arbetter, T. E., J. A. Curry, and J. A. Maslanik, On the effects of rheology

and ice thickness distribution in a dynamic-thermodynamic sea ice model, *J. Phys. Oceanogr.*, *29*, 2656–2670, 1999.

Arbetter, T. E., Development of an improved dynamic-thermodynamic sea ice thickness distribution model, Ph.D. dissertation, 192 pp., Univ. of Colo., Boulder, Colo., 1999.

Beesley, J. A., C. S. Bretherton, C. Jakob, E. L. Andreas, J. M. Intrieri, and T. A. Uttal, A comparison of cloud and boundary layer variables in the ECMWF forecast model with observations at Surface Heat Budget of the Arctic Ocean (SHEBA) ice camp, *J. Geophys. Res.*, 105, 12,337–12,349, 2000.

Cullather, R. I., D. H. Bromwich, and M. C. Serreze, The atmospheric hydrologic cycle over the Arctic basin from reanalyses, Part I, Comparison with observations and previous studies, *J. Clim.*, *13*, 923–937, 2000.

Curry, J. A., J. Schramm, and E. E. Ebert, On the sea ice albedo climate feedback mechanism, *J. Clim.*, *8*, 240–247, 1995.

Curry, J. A., J. L. Schramm, D. Perovich, and J. O. Pinto, Applications of SHEBA/FIRE data to evaluation of snow/ice albedo parameterizations, *J. Geophys. Res.*, *106*, 15,345–15,355, 2001.

Ebert, E. E., and J. A. Curry, An intermediate one-dimensional thermodynamic sea ice model for investigating ice-atmosphere interactions, *J. Geophys. Res.*, *98*, 10,085–10,109, 1993.

Flato, G. M., The role of dynamics in warming sensitivity of arctic sea ice models, paper presented at Workshop on Polar Processes in Global Climate, Am. Meterol. Soc., Cancun, Mexico, Nov. 13–15 1996.

Flato, G. M., and W. D. Hibler III, Ridging and strength in modeling the thickness distribution of Arctic sea ice, *J. Geophys. Res.*, *100*, 18,611–18,626, 1995.

Harder, M., P. Lemke, and M. Hilmer, Simulation of sea ice transport through Fram Strait: Natural variability and sensitivity to forcing, *J. Geophys. Res.*, *103*, 5595–5606, 1998.

Hibler, W. D., A dynamic thermodynamic sea ice model, *J. Phys. Oceanogr.*, *9*, 817–846, 1979.

Hilmer, R., M. Harder, and P. Lemke, Sea ice transport: A highly variable link between Arctic and North Atlantic, *Geophys. Res. Lett.*, *25*, 3359–3362, 1998.

Holland, M. M., and J. A. Curry, The role of physical processes in determining the interdecadal variability of central Arctic sea ice, *J. Clim.*, *12*, 3319–3330, 1999.

Holland, D. M., L. A. Mysak, D. K. Manak, and J. M. Oberhuber, Sensitivity study of a dynamic thermodynamic sea ice model, *J. Geophys. Res.*, *98*, 2561–2586, 1993.

Idso, S. B., and R. D. Jackson, Thermal radiation from the atmosphere, *J. Geophys. Res.*, *74*, 5397–5403, 1969.

Kalnay, E., et al., The NCEP/NCAR 40-year reanalysis project, *Bull. Am. Meterol. Soc.*, *77*(3), 437–471, 1996.

Kreyscher, M., M. Harder, P. Lemke, and G. M. Flato, Results of the Sea Ice Model Intercomparison Project: Evaluation of sea ice rheology schemes for use in climate simulations, *J. Geophys. Res.*, *105*, 11,299–11,320, 2000.

Lindsay, R., Ice deformation near SHEBA, *J. Geophys. Res.*, *107*, 10.1029/2000JC000445, in press, 2002.

Marshunova, M. S., Principle regularities of the radiation balance of the underlying surface and of the atmosphere in the Arctic (in Russian), *Tr. Arkt. Antarkt. Nauchno Issled. Inst.*, *229*(5), 51–103, 1961.

Maykut, G. A., and N. Untersteiner, Some results from a time-dependent thermodynamic model of sea ice, *J. Geophys. Res.*, *76*, 1550–1575, 1971.

Perovich, D. K., et al., Year on ice gives climate insights, *Eos Trans. AGU*, *80*(41), 481, 485–486, 1999.

Perovich, D. K., W. B. Tucker III, and K. A. Ligett, Aerial observations of the evolution of ice surface conditions during summer, *J. Geophys. Res.*, *107*, 10.1029/2000JC000449, in press, 2002.

Pinker, R. T., I. Laszlo, C. H. Whitlock, and T. P. Charlock, Radiative flux opens new window on climate research, *Eos Trans. AGU*, 76(15), 145, 155, 158, 1995.

Rigor, I., R. Colony, and S. Martin, Variations in surface air temperature observations in the Arctic 1979–1997, *J. Clim.*, *13*, 896–914, 2000.

Schramm, J. L., M. Holland, J. A. Curry, and E. E. Ebert, Modeling the thermodynamics of a distribution of sea ice thicknesses, 1, Sensitivity to ice thickness resolution, *J. Geophys. Res.*, *102*, 23,079–23,092, 1997a.

Schramm, J. L., M. M. Holland, and J. A. Curry, Applications of a single–column ice/ocean model understanding the mass balance of sea ice and snow in the central Arctic, *Ann. Glaciol.*, *25*, 287–291, 1997b.

Schweiger, J. A., and J. R. Key, Arctic Ocean radiative fluxes and cloud forcing estimated from the ISCCP C2 cloud dataset, 1983–1990, *J. Appl. Meteorol.*, *33*(8), 948–963, 1994.

Serreze, M. C., and C. M. Hurst, Representation of mean Arctic precipitation from NCEP-NCAR and ERA reanalysis, *J. Clim.*, *13*, 182–201, 2000.

Serreze, M. C., J. R. Key, J. E. Box, J. A. Maslanik, and K. Steffen, A new monthly climatology of global radiation for the Arctic and comparisons with NCEP-NCAR reanalysis and ISCCP-C2 fields, *J. Clim.*, *11*, 121–136, 1998.

Zhang, J., and D. Rothrock, Surface downwelling radiative fluxes: Ice model sensitivities and data accuracies, paper presented at Workshop on Polar Processes in Global Climate, Am. Meteorol. Soc., Cancun, Mexico, Nov. 13–15 1996.

Zhang, J., D. A. Rothrock, and M. Steele, Warming of the Arctic Ocean by a strengthened Atlantic inflow: Model results, *Geophys. Res. Lett.*, *25*, 1745–1748, 1998. (Correction, *Geophys. Res. Lett.*, *25*, 3541, 1998).

Zillman, J. W., A study of some aspects of the radiation and heat budgets of the Southern Hemisphere oceans, in *Meteorological Studies, Rep. 26*, 562 pp., Bur. of Meteorol., Dep. of Inter., Canberra, Australia, 1972.

A. Alam, T. E. Arbetter, J. A. Curry, R. Reeder, and J. L. Schramm, Program in Atmospheric and Oceanic Sciences, Department of Aerospace Engineering Sciences, University of Colorado, Campus Box 429, Boulder, CO 80309, USA. (afshan.alam@colorado.edu; todd.arbetter@colorado.edu; curryja@cloud.colorado.edu; randolph.reeder@colorado.edu; schramm@ucar.edu)

P. Guest, Department of Meteorology, Naval Postgraduate School, 589 Dyer Road, Room 254, Monterey, CA 93943 5114, USA. (pguest@nps.navy.mil)